

Fully robust qubit in atomic and molecular three-level systems

N. Aharon¹, I. Cohen¹, F. Jelezko^{2,3}, and A. Retzker¹

¹*Racah Institute of Physics, The Hebrew University of Jerusalem, Jerusalem 91904, Givat Ram, Israel*

²*Center for Integrated Quantum Science and Technology, Universität Ulm, D-89081 Ulm, Germany*

³*Institut für Quantenoptik, Albert-Einstein Allee 11, Universität Ulm, D-89081 Ulm, Germany*

We present a new method of constructing a fully robust qubit in a three-level system. By the application of continuous driving fields, robustness to both external and controller noise is achieved. Specifically, magnetic noise and power fluctuations do not operate within the robust qubit subspace. Whereas all the continuous driving based constructions of such a fully robust qubit considered so far have required at least four levels, we show that in fact only three levels are necessary. This paves the way for simple constructions of a fully robust qubit in many atomic and solid state systems that are controlled by either microwave or optical fields. We focus on the NV-center in diamond and analyze the implementation of the scheme, by utilizing the electronic spin sub-levels of its ground state. In current state-of-the-art experimental setups the scheme leads to improvement of more than two orders of magnitude in coherence time, pushing it towards the lifetime limit. We show how the fully robust qubit can be used to implement quantum sensing, and in particular, the sensing of high frequency signals.

PACS numbers: 03.67.Ac, 03.67.Pp

I. INTRODUCTION

The implementation of quantum technology applications and quantum information processing requires a reliable realization of qubits that can be initialized, manipulated, and measured efficiently. In solid state and atomic systems, ambient magnetic field fluctuations constitute a serious impediment, which usually limits the coherence time to several orders of magnitude less than the lifetime limit. Pulsed dynamical decoupling [1–3] has proven to be very useful in prolonging the coherence time [4–11]. However, in order to mitigate both external and controller noise, very rapid and composite pulse sequences must be applied [12–16], which are not easily incorporated into other operations and require a lot of power [17]. Similarly, in continuous dynamical decoupling [17–25], the effect of the controller noise can be diminished by either a rotary echo scheme [26, 27], which is then analogous to pulsed dynamical decoupling, or by the concatenation of several driving fields [28–30], which is limited by the reduction of the dressed energy gap, and results in slower qubit gates. However, a multi-state system enables a different approach. In [31], a fully robust qubit; i.e., a qubit that is robust to both external and controller noise, was realized by the application of continuous driving fields on a specific hyperfine structure. Subsequently, a general scheme for the construction of a fully robust qubit was introduced in [32].

So far, all the continuous driving based implementations of a fully robust qubit have been investigated [32–36] and experimentally realized [31, 37–40] with the application of on-resonance driving fields. This, however, requires at least four energy levels on which the driving fields operate, and hence is not applicable to a three-level system. In fact, together with a three-level system, an additional hyperfine level was considered in [31]. In [34], one of the excited states of the NV-center was used, but necessitated a cryogenic temperature, and in [32] two Λ systems (composed of six states) were employed.

In this paper we show how a fully robust qubit can be constructed by only utilizing a three-level system through the application of continuous *off-resonant* driving fields. Our

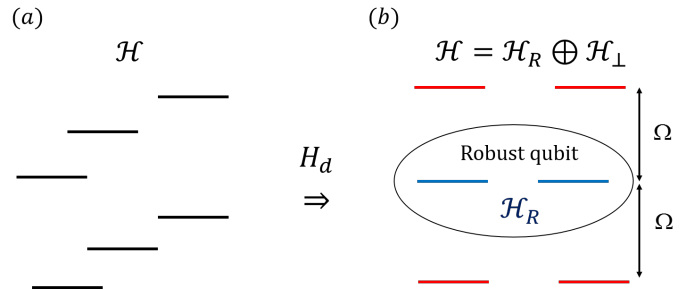


Figure 1. **Fully robust qubit.** By the application of continuous driving fields we create a robust qubit subspace. Magnetic noise and power fluctuations of the driving fields do not operate within the robust qubit subspace. (a) Bare states, H_d (driving Hamiltonian). (b) Fully robust qubit (blue), Ω (smallest energy gap between the robust qubit states and non-robust states).

method achieves robustness to driving noise, which is the typical problem of continuous dynamical decoupling schemes. Three level-systems are widely available and appear in many atomic and solid state systems, such as trapped ions, rare-earth ions, defect centers, and in particular, the NV-center in diamond. This scheme is applicable to both optical and microwave configurations. The fact that only the three-level system is manipulated facilitates the realization of the fully robust qubit and its integration in the target application. Moreover, the construction by off-resonant driving fields enables the implementation of fast, simple qubit gates. Our scheme is therefore aimed at enhancing the performance of a wide range of tasks in the fields of quantum information science and quantum technologies, and in particular, quantum sensing, where due to the off-resonance construction, our scheme constitutes a novel method for sensing high frequency signals.

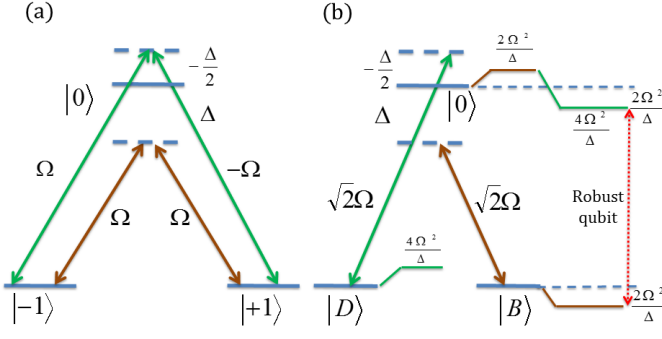


Figure 2. **Fully robust qubit in a three-level system.** (a) Two Λ systems are created via the same level with two unequal detunings of opposite signs. (b) The driving fields of the two Λ systems result in Stark shifts of the three levels, here described in the $\{|B\rangle, |D\rangle, |0\rangle\}$ basis. In the case where the ratio between the red detuning and the blue detuning is equal to 2 (and for the specific values of the Rabi frequencies), the Stark shifts of the $|B\rangle$ and $|0\rangle$ states are identical. At the same time, a large energy gap is formed between the $|B\rangle$ and $|D\rangle$ states.

II. FULLY ROBUST QUBIT

We start with an explicit definition of a fully robust qubit [32]. Let us denote by $\{|R_i\rangle\}$ the robust qubit states. In what follows H_d is the (continuous) driving Hamiltonian, \mathcal{H}_R is the Hilbert subspace of the fully robust qubit, and \mathcal{H}_\perp is the complementary Hilbert space, that is, $\mathcal{H} = \mathcal{H}_R \oplus \mathcal{H}_\perp$. We define the fully robust qubit by (See Fig. 1)

$$\langle R_i | S_z | R_j \rangle = 0 \quad \forall i, j, \quad (1)$$

$$H_d |R_i\rangle = \lambda^R |R_i\rangle \quad \forall i. \quad (2)$$

The first equation ensures that magnetic noise does not operate within the subspace of the fully robust qubit; the noise can only cause transitions between a robust state and a state in the complementary subspace. We assume (by construction) that the energy of all states in \mathcal{H}_R is far from the energy of the states in \mathcal{H}_\perp . More specifically, we assume that $\nu = \min_i |\lambda_i^\perp - \lambda^R|$, where λ^R (λ_i^\perp) is an eigenvalue of an eigenstate in \mathcal{H}_R (\mathcal{H}_\perp), is much larger than the characteristic frequency of the noise, as in this case the lifetime T_1 would be inversely proportional to the power spectrum of the noise at ν . This ensures that the rate of transitions from \mathcal{H}_R to \mathcal{H}_\perp due to magnetic noise is negligible.

The second equation indicates that the robust states do not collect a relative dynamical phase due to H_d , and are therefore immune to noise originating from H_d . Power fluctuations of the driving fields result in identical energy fluctuations of the robust states.

To summarize, the first equation ensures that the robust states are immune to external noise, while the second equation ensures that the robust states are also immune to controller noise.

III. FULLY ROBUST QUBIT IN A THREE-LEVEL SYSTEM

The rationale for the method is illustrated in Fig. 2. Driving a three-level system in a Λ configuration with large detunings results in Stark shifts of all three levels. We design the driving fields; i.e., their Rabi frequencies and detunings, in such a way that the new eigenstates are decoupled, in first order, from the external magnetic field (see Eq. 1). In addition, up to the second order, two of the eigenstates have an identical Stark shift (see Eq. 2); hence, fluctuations in the energy gap between them are mitigated since noise in the driving fields will cause only fluctuations due to the higher order terms of the Stark shifts. Specifically, we consider driving fields in two Λ configurations. In one Λ configuration the driving fields are red detuned and in the second Λ configuration the driving fields are blue detuned. Denote by Ω the Rabi frequency of the driving fields, and by Δ the detuning. The red detuned driving fields, which correspond to (in the interaction picture (IP))

$$H^{red} = \Omega \left(|0\rangle \langle -1| e^{-i\Delta t} + |0\rangle \langle +1| e^{-i\Delta t} \right) + h.c., \quad (3)$$

result in the effective Hamiltonian [41]

$$H_{eff}^{red} = -\frac{\Omega^2}{\Delta} (2S_x^2 + 4S_z^2 - 4\mathbf{1}). \quad (4)$$

Similarly, the blue detuned driving fields, which correspond to

$$H^{blue} = \Omega \left(|0\rangle \langle -1| e^{+i\frac{\Delta}{2}t} - |0\rangle \langle +1| e^{+i\frac{\Delta}{2}t} \right) + h.c., \quad (5)$$

result in the effective Hamiltonian

$$H_{eff}^{blue} = -\frac{\Omega^2}{\Delta} (4S_x^2 - 4S_z^2). \quad (6)$$

Our construction therefore results in the effective Hamiltonian

$$H_{eff} = H_{eff}^{red} + H_{eff}^{blue} = -\frac{\Omega^2}{\Delta} (6S_x^2 - 4\mathbf{1}), \quad (7)$$

whose $|B\rangle = \frac{1}{\sqrt{2}}(|+1\rangle + |-1\rangle)$ and $|0\rangle$ eigenstates have a zero first order Zeeman shift and identical energies. Hence, the two requirements for a fully robust qubit, Eq. 1 and Eq. 2, are fulfilled by the $|B\rangle$ and $|0\rangle$ states (with $H_d = H_{eff}$). Viewed in the $\{|B\rangle, |D\rangle, |0\rangle\}$ basis, where $|D\rangle = \frac{1}{\sqrt{2}}(|+1\rangle - |-1\rangle)$, the red detuned driving fields induce a positive (negative) Stark shift to the $|0\rangle$ ($|B\rangle$) state, while the blue detuned driving fields induce a negative (positive) Stark shift to the $|0\rangle$ ($|D\rangle$) state. The driving fields are therefore tuned such that the total Stark shift of the $|0\rangle$ state will be equal to the Stark shift of the $|B\rangle$ state (see Fig. 2).

We assume a zero-field splitting between the $|0\rangle$ and $|\pm 1\rangle$ states. In case that the $|\pm 1\rangle$ states are split, due to a static magnetic field, the on-resonance frequencies of the $|-1\rangle \leftrightarrow |0\rangle$ and $|+1\rangle \leftrightarrow |0\rangle$ transitions are not identical, therefore, we

consider the regime where $g\mu_B B \gg \Delta \gg \Omega$. Hence, each Λ system requires two different (phase-matched) driving fields and, in the case of a microwave implementation (with linear polarizations), corrections on the order of $\sim \frac{\Omega^2}{g\mu_B B}$ are introduced.

IV. ROBUSTNESS

We first analyze the robustness of the scheme to environmental and controller noise, which are extremely crucial to the NV-based implementation, and then refer to possible errors in the general experimental set-up.

With respect to environmental noise, dephasing of the dressed states is caused by two factors. The first source of dephasing is the high order coupling to the external magnetic field. By construction, the first order coupling is eliminated, but higher order terms remain. This can be grasped by moving to the time independent frame of the dressed states. In the lab frame, and in the basis of the bare states, the Hamiltonian of the noise is given by

$$H_{noise} = g\mu_B B(t)S_z, \quad (8)$$

where $B(t)$ is a randomly fluctuating magnetic field. Moving to the IP with respect to the energies of the bare states, and then moving to the basis of the dressed states, H_{noise} is transformed to

$$H_{noise}^I = g\mu_B B(t)(|B\rangle\langle D| + h.c.). \quad (9)$$

We continue by moving to the time independent frame; that is, to the IP with respect to $H_0^I = -\Delta|B\rangle\langle B| + \frac{\Delta}{2}|D\rangle\langle D|$. This results in

$$H_{noise}^{II} = g\mu_B B(t)(|B\rangle\langle D|e^{-i\frac{3}{2}\Delta t} + h.c.). \quad (10)$$

The Stark shifts obtained by the driving fields are accompanied by a small amplitude mixing between the ideal $\{|0\rangle, |B\rangle, |D\rangle\}$ states (i.e., the exact eigenstates), which means that H_{noise}^{II} is further (slightly) rotated to have both diagonal and other off-diagonal terms. However, due to the high detuning of $\sim \frac{3}{2}\Delta$, the effect of all of these contributions is negligible. Therefore, the significant effect of the noise is due to the coupling between the $|B\rangle$ and $|D\rangle$ states. In the first order, the noise induces a longitudinal relaxation (decay) rate of $\sim S_{BB}(E_{BD})$, where S_{BB} is the power spectrum of the noise, and E_{BD} is the energy gap between the $|B\rangle$ and $|D\rangle$ states. Hence, a large E_{BD} ensures that the longitudinal relaxation rate is negligible ($\sim S_{BB}(E_{BD}) \ll \frac{1}{T_1}$). In this case, the noise does not induce transitions between the $|B\rangle$ and $|D\rangle$ states, but does result in a second order fluctuating phase shift of $\sim \frac{(g\mu_B B(t))^2}{E_{BD}}$. The resulting dephasing rate is considerably diminished with an increasing E_{BD} (see Appendix A). The second source of dephasing is due to the counter-rotating terms of the driving fields, which induce minor mixing between the $|B\rangle$ and $|D\rangle$ states via a Raman transition. In case that the $|\pm 1\rangle$ states are Zeeman sub-levels, this results in an additional mixing term of $\sim (\frac{\Omega^2}{g\mu_B B})S_z$ in the effective Hamiltonian of Eq. (7),

and the mixing is of the order of $\sim (\frac{\Omega^2}{g\mu_B B})/(\frac{\Omega^2}{\Delta}) = \frac{\Delta}{g\mu_B B}$. This implies a dephasing rate of $\sim \frac{\Delta}{g\mu_B B}S_{BB}(0)$, which is greatly suppressed by enlarging the Zeeman splitting.

Regarding controller noise, in an ideal construction the (second order) Stark shifts of the $|B\rangle$ and $|0\rangle$ states are identical and therefore immunity to controller noise is obtained. However, while we can fix the second order Stark shifts to be identical, the fourth order terms might not be negligible, and in this case will introduce an energy gap between the $|B\rangle$ and $|0\rangle$ states. Fluctuations of this energy gap, due to driving amplitude noise, can be significantly reduced by either an exact calculation of the fourth order energy shifts, or a numerical search for the point of a non-zero second order shift, which is robust to driving fluctuations [44]. In Appendix B we show how robustness could be further improved by utilizing a double-drive, where the first drive is on-resonance and the second drive is off-resonance.

For the case of an NV-center in diamond, which we analyzed in detail (see below), our scheme achieves a significant improvement in the coherence time under realistic conditions that take into account both environmental noise and power fluctuations of driving fields.

The robustness of the scheme may also be affected by errors in the experimental set-up. An uncertainty, or a drift, of the static magnetic field, δB_z , shifts the bare $|+1\rangle$ and $|-1\rangle$ states, and therefore introduces two-photon detunings. Compared to the effect of the fluctuating magnetic noise, the dominant effect here is a first order effect. The coupling between the $|B\rangle$ and $|D\rangle$ states results in an amplitude mixing and the $|B\rangle$ state is modified to $|\tilde{B}\rangle \sim |B\rangle + \frac{g\mu_B \delta B_z \Delta}{\Omega^2}|D\rangle$. Hence, δB_z inflicts a dephasing rate of $\sim \frac{g\mu_B \delta B_z \Delta}{\Omega^2}S_{BB}(0)$. This dephasing rate, however, remains negligible as long as the energy gap between the dressed states is much larger than the magnetic field uncertainty; that is, $\frac{\Omega^2}{\Delta} \gg g\mu_B \delta B_z$. In addition, there can be relative amplitude and relative phase errors between the two driving fields of a Λ system. In both cases, a relative error of ε will introduce an amplitude mixing of $\sim \frac{\varepsilon\Omega}{\Delta}$ and an energy shift of $\sim \frac{\varepsilon^2\Omega^2}{\Delta}$. For example, a relative amplitude error of ε in the red detuned Λ system introduces (in the IP) the coupling term $\varepsilon\Omega(|0\rangle\langle D|e^{-i\frac{3}{2}\Delta t} + h.c.)$, which results in an amplitude mixing of $\sim \frac{\varepsilon\Omega}{\Delta}$ between the $|0\rangle$ and $|D\rangle$ states. Since the magnetic noise rotates at the same frequency as this coupling term (see Eq. 10) and because there is an amplitude mixing of $\sim \frac{\Omega}{\Delta}$ between the $|0\rangle$ and $|B\rangle$ states, we have that $\langle 0|S_z|0\rangle \sim (\frac{\Omega}{\Delta})^2\varepsilon$, and hence, the inflicted dephasing rate due to a relative amplitude error of ε is $\sim (\frac{\Omega}{\Delta})^2\varepsilon S_{BB}(0)$.

V. SINGLE QUBIT GATES

In this section we show how protected qubit gates can be implemented and discuss their application for sensing. A σ_x gate can be realized by driving the $|B\rangle \leftrightarrow |0\rangle$ transition on

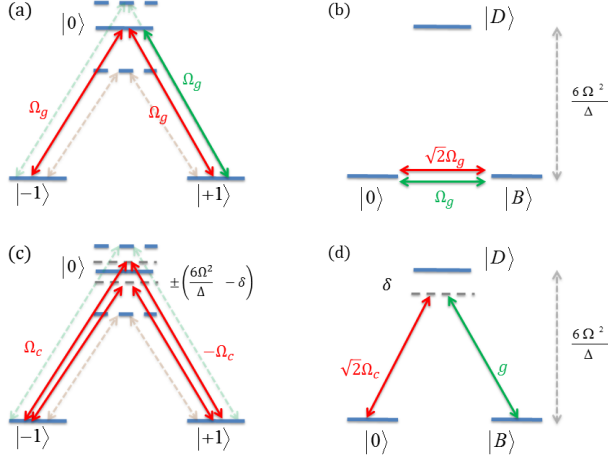


Figure 3. **Single qubit gate and sensing.** A single qubit gate in the bare states basis (a), and in the dressed states basis (b). Red (green) arrows correspond to a gate with $\Omega_g \ll \Delta$ ($\Omega_g \ll \frac{\Omega^2}{\Delta}$). The green gate enables the sensing of high frequency fields. (c) Control field used for the sensing of low frequency fields via a Raman transition in the bare states basis. (d) The sensing Raman transition in the dressed states basis, where g denotes the sensing field. Dashed arrows in (a) and (c) represent the dressing driving fields.

resonance with

$$H_x = \Omega_g (\cos(\omega_{-1,0}t) |0\rangle\langle -1| + \cos(\omega_{+1,0}t) |0\rangle\langle +1|) + h.c.. \quad (11)$$

Note that while a concatenated on-resonance driving scheme allows for slow gates with $\Omega_g \ll \Omega_n$, where Ω_n is the Rabi frequency of the last driving field, our method enables fast gates, where Ω_g is limited solely by the detuning, $\Omega_g \ll \Delta$ (see Fig. 3). A σ_y gate can be realized by introducing a phase shift of $\frac{\pi}{2}$ in the driving frequency with respect to the driving frequency of the σ_x gate. Alternatively, one can start with a polarization that corresponds to the σ_y gate, and then add the $\frac{\pi}{2}$ phase shift to get the σ_x gate. These realizations of σ_x or σ_y gates require two (phase-matched) driving fields, which only couple the $|B\rangle$ state to the $|0\rangle$ state (similar to the dressing fields). A simpler implementation of the gates can be achieved by employing only one of the driving fields. However, as this driving field couples both the $|B\rangle$ and $|D\rangle$ states to the $|0\rangle$ state, Ω_g is limited by $\Omega_g \ll \frac{\Omega^2}{\Delta}$.

VI. SENSING

Sensing of high frequency signals is of great importance, especially in the case of classical fields sensing [45, 46], in detection of electron spins in solids [47] and NMR [48]. To the best of our knowledge, to date, dynamical decoupling techniques have not been incorporated in sensing schemes of high frequency signals, which are therefore limited by T_2^* . Our scheme enables enhanced sensing of high frequency AC signals, where a signal induces rotations of the fully robust qubit.

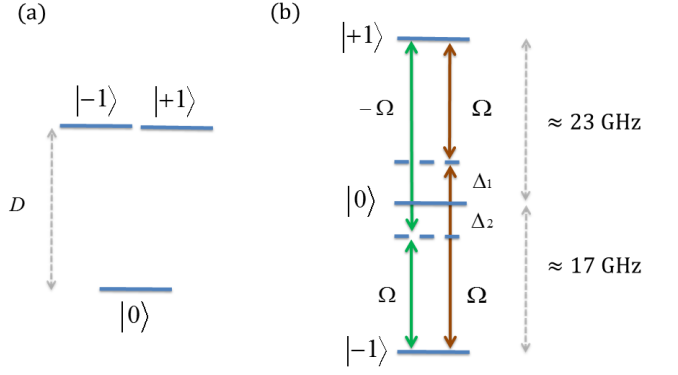


Figure 4. **Implementation with the NV-center.** Ground state of the NV-center. (a) Without a static magnetic field. (b) With a static magnetic field and driving fields. The ratio of Δ_1 to Δ_2 is chosen such that robustness to power fluctuations of driving fields is achieved.

This can be accomplished by tuning the frequency of the $|B\rangle \leftrightarrow |0\rangle$ transition to the sensing field frequency, as in this case the frequency corresponds to the energy gap between the bare $|0\rangle$ and $|\pm 1\rangle$ states. Since the sensing sensitivity scales, in the shot noise limit, like $\sqrt{T_2}$, for the case of sensing with an NV-center our scheme predicts an improvement of ~ 1 order of magnitude in sensitivity.

Sensing of AC signals with lower frequencies can be done by a Raman transition. We assume that the AC signal corresponds to a σ_z operation, which couples the $|B\rangle$ and $|D\rangle$ states, and its amplitude is denoted by g . A Raman transition between the $|B\rangle$ and $|0\rangle$ states is achieved by adding a control field whose frequency is tuned to match the same detuning as that of the AC signal, so a one-photon detuning is obtained (See Fig. 3 (c), (d)). Full oscillation will then be observed whenever $\sqrt{2}\Omega_c = g$, where Ω_c is the Rabi frequency of the control field. In this case the sensing sensitivity is limited by the fluctuations of the (dressing) Rabi frequency, Ω , which results in fluctuations of the one-photon detuning, δ . Ideally, the sensitivity scales like $\frac{\delta}{g} \sqrt{T_2^\Omega}$, where T_2^Ω is the coherence time induced by the Rabi frequency fluctuations. Note that the sensitivity of low-frequency signal sensing using the bare state scales like $\sqrt{T_2^*}$, while a scaling of $\sqrt{T_2^\Omega}$ is obtained by utilizing the $|B\rangle \leftrightarrow |D\rangle$ transition of the dressed states.

VII. IMPLEMENTATION WITH THE NV-CENTER IN DIAMOND

The electronic ground state of the NV-center is a spin 1 state, where the $|\pm 1\rangle$ states are separated from the $|0\rangle$ state by a zero-field splitting of $D = 2.87$ GHz [49, 50] (see Fig. 4 (a)). We consider a static magnetic field, which is applied along

the NV axis, such that $g\mu_B B \approx 20$ GHz (note that a larger Zeeman splitting would result in a better decoupling from the magnetic noise). In this case level-crossing occurs and the energy gaps between $|0\rangle$ and $|\pm 1\rangle$ correspond to $\omega_{0,+1} \approx 23$ GHz and $\omega_{0,-1} \approx 17$ GHz (see Fig. 4 (b)). We assume that to have a good decoupling of the robust qubit and the magnetic noise we need to create an energy gap of $\gtrsim 10$ MHz between the $|B\rangle$ and $|D\rangle$ states; hence, we set $\Omega = 70$ MHz [51, 52]. This implies that the conditions for an ideal construction, $g\mu_B B, \omega_0 \gg \Delta \gg \Omega$, are not fully satisfied and therefore the Stark shifts will have contributions from all driving fields as well as from the counter-rotating terms. The Hamiltonian of the system is given by

$$H = \omega_0 S_z^2 + \omega_B S_z + \Omega S_x \left(\cos[(\omega_0 + \omega_B - \Delta_1)t] + \cos[(\omega_0 - \omega_B - \Delta_1)t] + \cos[(\omega_0 + \omega_B + \Delta_2)t] - \cos[(\omega_0 - \omega_B + \Delta_2)t] \right), \quad (12)$$

where $\omega_0 = D$ and $\omega_B = g\mu_B B$. By moving to the IP with respect to $H_0 = \omega_0 S_z^2 + \omega_B S_z$ (but not taking the rotating-wave approximation (RWA)), and then moving to the ideal dressed states basis, $\{|0\rangle, |B\rangle, |D\rangle\}$ we obtain $H_I = U e^{iH_0 t} H e^{-iH_0 t} U^\dagger$, from which we calculate, in the ideal dressed states basis, the energy shifts of the dressed states (up to the second order) [41, 42]. The energy shifts are given by [43]

$$\Delta E_B = \frac{1}{8} \Omega^2 \left(\frac{4}{\Delta_1} + \frac{4}{2\omega_0 - \Delta_1} + \frac{1}{2\omega_B + \Delta_1} - \frac{1}{2\omega_B - \Delta_1} + \frac{1}{2\omega_B - \Delta_2} - \frac{1}{2\omega_B + \Delta_2} + \frac{1}{-2\omega_B - \Delta_1 + 2\omega_0} + \frac{1}{2\omega_B - \Delta_1 + 2\omega_0} + \frac{1}{-2\omega_B + \Delta_2 + 2\omega_0} + \frac{1}{2\omega_B + \Delta_2 + 2\omega_0} \right), \quad (13)$$

$$\Delta E_D = \frac{1}{8} \Omega^2 \left(-\frac{4}{\Delta_2} + \frac{4}{2\omega_0 + \Delta_2} + \frac{1}{2\omega_B - \Delta_2} - \frac{1}{2\omega_B + \Delta_2} + \frac{1}{2\omega_B + \Delta_1} - \frac{1}{2\omega_B - \Delta_1} + \frac{1}{-2\omega_B + \Delta_2 + 2\omega_0} + \frac{1}{2\omega_B + \Delta_2 + 2\omega_0} + \frac{1}{-2\omega_B - \Delta_1 + 2\omega_0} + \frac{1}{2\omega_B - \Delta_1 + 2\omega_0} \right), \quad (14)$$

$$\Delta E_0 = -\Delta E_B - \Delta E_D. \quad (15)$$

In an ideal scenario the terms $\sim \frac{\Omega^2}{\omega_0}, \frac{\Omega^2}{\omega_B}$ would be negligible, and hence, the requirement $\Delta E_0 = \Delta E_B$ would imply $\Delta_2 = \frac{\Delta_1}{2}$.

In order to achieve an energy gap of $\gtrsim 10$ MHz between the $|B\rangle$ and $|D\rangle$ states, together with $\Omega = 70$ MHz, we also set $\Delta_1 = 500$ MHz. For $\Delta E_0 = \Delta E_B$, the energy gap between the $|0\rangle$ and $|B\rangle$ states, due to the fourth order energy shifts, is $E_{0B} = E_0 - E_B \approx 0.25$ MHz, which means that driving fluctuations will impose a limitation on the coherence time. We therefore tune the energy shifts to a robust point at which $\Delta E_0 - \Delta E_B \approx 0.63$ MHz, and $E_{0B} \approx 0.315$ MHz [44]. In

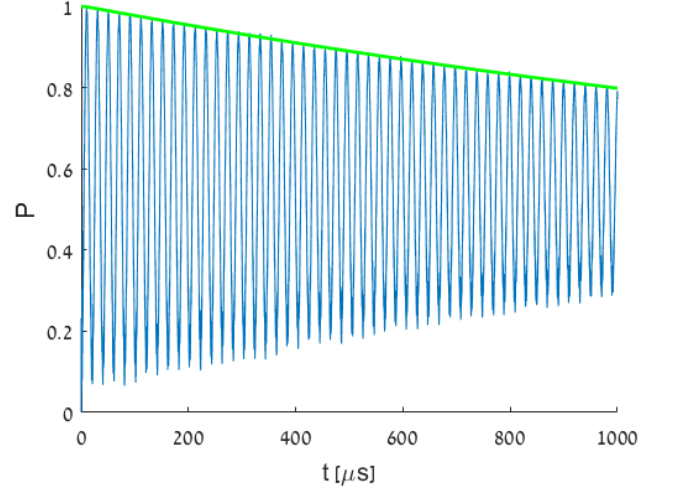


Figure 5. **Coherence time.** Simulation of an NV-center implementation of a fully robust qubit where $T_2^* = 5 \mu s$, $\Omega = 70$ MHz, $\Delta_1 = 500$ MHz and $\Delta_2 = 209$ MHz. The graph is a result of average over 200 trails, and shows oscillations between the $|\psi_{\pm}\rangle = \frac{1}{\sqrt{2}}(|0\rangle \pm |B\rangle)$ states. The theoretical dephasing rate is plotted in green and corresponds to a coherence time of $T_2 \simeq 1820 \mu s$.

this case we have that $\Delta_1 = 500$ MHz, $\Delta_2 \approx 209$ MHz, and $E_{BD} \approx 17.96$ MHz.

We verified the robustness of this scheme by simulating its performance when the NV spin was subject to magnetic noise and driving fluctuations. We modelled the magnetic noise, $B(t)$, as an Ornstein-Uhlenbeck process [53, 54] with a zero expectation value, $\langle B(t) \rangle = 0$, and a correlation function $\langle B(t)B(t') \rangle = \frac{c\tau}{2} e^{-\gamma|t-t'|}$. An exact simulation algorithm [55] was employed to realize the Ornstein-Uhlenbeck process, which according to

$$B(t + \Delta t) = B(t)e^{-\frac{\Delta t}{\tau}} + n\sqrt{\frac{c\tau}{2}} \left(1 - e^{-\frac{2\Delta t}{\tau}}\right), \quad (16)$$

where n is a unit Gaussian random number. We took the pure dephasing time to be $T_2^* = 5 \mu s$, and the correlation time of the noise was set to $\tau = \frac{1}{\gamma} = 15 \mu s$ [56, 57], where the diffusion constant is given by $c \approx \frac{4}{T_2^* 2\tau}$. Driving fluctuations were also modelled by an Ornstein-Uhlenbeck process with a zero expectation value. We chose a correlation time of $\tau_{\Omega} = 500 \mu s$, and a relative amplitude error of $\delta_{\Omega} = 0.5\%$ so the diffusion constant is given by $c_{\Omega} = 2\delta_{\Omega}/\tau_{\Omega}$. Fig. 5 presents the outcome of the simulation of the fully robust qubit under the effect of magnetic and driving noise. The plot shows oscillations between the $|\psi_{\pm}\rangle = \frac{1}{\sqrt{2}}(|0\rangle \pm |B\rangle)$ states averaged over 200 trials. The oscillations are not symmetric because fast oscillations due to counter-rotating terms at (local) minimum values of P are averaged to zero. The simulation confirmed our estimation of $T_2 \simeq 1820 \mu s$, an improvement of more than 2 orders of magnitude in the coherence time, pushing it towards the lifetime limit. Note that the simulation does not take decoherence due to longitudinal spin re-

laxation (of the bare states) into account, which is given by $\Gamma_2 = \frac{\Gamma_1}{2}$, where $\Gamma_1 = \frac{1}{T_1}$ (since $S_{BB}(E_{BD}) \ll \Gamma_1$, the effect of the noise on the life time of the dressed states is negligible).

The probability of remaining in the initial $|\psi_+\rangle$ state is given by (green line in Fig. 5)

$$P = \frac{1 + |F(t)G(t)|e^{-\gamma_m t} e^{-(\gamma_d t)^2}}{2}, \quad (17)$$

where

$$F(t, \Omega) = \frac{\exp\left(\frac{\gamma}{2}\right)}{\sqrt{\cosh\left(\frac{\xi t}{2}\right) + \frac{2\gamma}{\xi} \sinh\left(\frac{\xi t}{2}\right)}}, \quad (18)$$

$$G(t, \Omega) = \exp\left(\frac{2ig^2}{\Omega\left(2\gamma + \xi \coth\left(\frac{\xi t}{2}\right)\right)}\right), \quad (19)$$

and

$$\xi = \sqrt{4\gamma^2 - \frac{16i\gamma g^2}{\Omega}}. \quad (20)$$

$|F(t)G(t)|$ corresponds to the (second order) dephasing due to the coupling between $|B\rangle$ and $|D\rangle$ (see Appendix A), $\gamma_m = \langle B|S_z|B\rangle S_{BB}(0)$ is the (first order) dephasing rate due to the amplitude mixing between $|B\rangle$ and $|D\rangle$, and $\gamma_d = \frac{\delta_r \delta_\Omega \Omega}{\sqrt{2}}$ is the dephasing rate due to driving fluctuations, where $\delta_r = \frac{|E_{0B}(\Omega + \delta\Omega) - E_{0B}(\Omega)|}{E_{0B}(\Omega)}$. In our case we estimated that $\gamma_m \approx 200\text{Hz}$, $\gamma_d = 182\text{Hz}$, and the coherence time due to the coupling between $|B\rangle$ and $|D\rangle$ alone is $\simeq 3440\mu\text{s}$. In Appendix C we show the effect of these different sources of noise on the coherence time, which together result in $T_2 = 1820\mu\text{s}$.

We used our theoretical model to estimate the achievable coherence times in different scenarios. Fig. 6 shows the estimated coherence times for the case of $T_2^* = 3\mu\text{s}$ as function of the correlation time of the noise and for various values of the Zeeman splitting. The parameters chosen for these estimations (see Appendix D) were not optimized and thus the obtained T_2 times constitute a lower bound estimation. Nevertheless, the estimations imply that a significant improvement in the coherence time can be achieved under even more severe conditions.

VIII. CONCLUSION

We presented a new method that enables the construction of a fully robust qubit utilizing a three-level system alone. By the application of off-resonance continuous driving fields in a Λ configuration, robustness to both external and controller noise is achieved. We analyzed the NV-center based implementation of the scheme and showed that with current state-of-the-art experimental setups the scheme enables an improvement of more than two orders of magnitude in the coherence time. Moreover, since the scheme allows for fast gates, it is advantageous with respect to on-resonance driving schemes, since

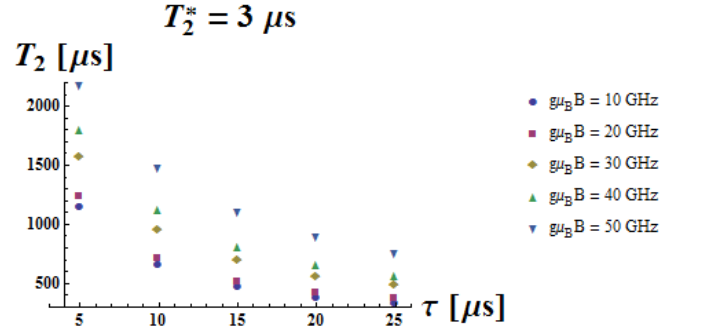


Figure 6. **Lower bound estimation of T_2 .** A theoretical (non-optimized) estimation of the coherence times for the case of $T_2^* = 3\mu\text{s}$ as function of the correlation time of the noise and for various values of the Zeeman splitting.

more qubit operations in a given T_2 time interval can be performed. Our analysis of the NV-center based implementation considered linearly polarized fields. The performance of the scheme is likely to be further improved by the application of circularly polarized fields [58]. This scheme is relevant to many tasks in the fields of quantum information science and quantum technologies, and in particular to quantum sensing of high frequency signals. The utilization of off-resonance driving fields makes the scheme more robust to an inhomogeneous broadening than schemes that use (continuous) on-resonance driving fields, and hence, it is more attractive for ensemble-based sensing. Our scheme is expected to perform even better in the optical regime, where large energy gaps, stronger driving fields, and polarization dependent transitions allow for much smaller mixing amplitudes between the ideal dressed states. Although here we considered the case of a spin 1 system, the scheme is also applicable to systems of half-integer spins. For example, in the case of the calcium ion, $^{40}\text{Ca}^+$, one could consider a Λ system composed of the $|S_{1/2}; +1/2\rangle$, $|D_{3/2}; -1/2\rangle$, $|D_{3/2}; +3/2\rangle$ states. In this case a fully robust optical qubit can be realized with $|0\rangle = |S_{1/2}; +1/2\rangle$ and $|B\rangle = \sqrt{\frac{1}{8}}|D_{3/2}; -1/2\rangle + \sqrt{\frac{7}{8}}|D_{3/2}; +3/2\rangle$.

ACKNOWLEDGMENTS

A. R. acknowledges the support of the Israel Science Foundation (grant no. 039-8823), the support of the European commission (STREp EQUAM Grant Agreement No. 323714), EU Project DIADEMS, the Marie Curie Career Integration Grant (CIG) IonQuanSense(321798), the Niedersachsen-Israeli Research Cooperation Program and DIP program (FO 703/2-1). This work was [partially] supported by the US Army Research Office under Contract W911NF-15-1-0250. This project has received funding from the European Union as part of the Horizon 2020 research and innovation program under grant agreement No. 667192. F. J. acknowledges the support of ERC, EU projects SIQS and DIADEMS, VW Stiftung, DFG and BMBF.

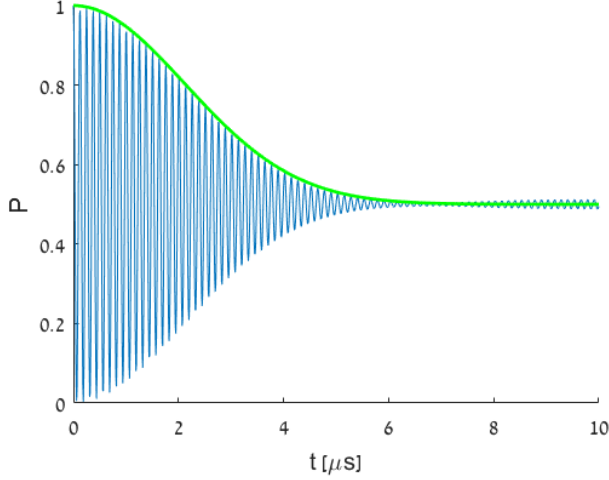


Figure 7. Simulation of pure dephasing with no driving fields. $\frac{1+e^{-\frac{g^2 t}{2}}}{2}$ is plotted in green ($g^2 = \frac{2}{T_2^2}$).

Appendix A

Here we analyze the dephasing of a strongly driven system. We consider the case of a two-level system (TLS) under a single on-resonance driving and magnetic noise. The Hamiltonian is given by

$$H = \frac{\omega_0}{2} \sigma_z + \Omega \cos(\omega_0 t) \sigma_x + B(t) \sigma_z,$$

where $B(t)$ is the random magnetic noise (here in units of frequency). Moving to the interaction picture (IP) with respect to $H_0 = \frac{\omega_0}{2} \sigma_z$, taking the rotating-wave-approximation (RWA), and moving to the dressed states basis, we get that

$$H_I = \frac{\Omega}{2} \sigma_z + B(t) \sigma_x.$$

In the regime of a strong driving field, $\Omega \gg |B(t)|$, the time evolution of the dressed states can be simplified by the adiabatic approximation and hence, the dressed states accumulate a phase which is given by

$$\phi(t) = \pm \frac{1}{2} \int_0^t dt' \sqrt{4B^2(t') + \Omega^2} \approx \pm \frac{1}{2} \int_0^t dt' \left(\Omega + \frac{2B^2(t')}{\Omega} \right)$$

We assume that $B(t)$ is an Ornstein-Uhlenbeck random process [53, 54], which is described by the stochastic differential equation

$$dB_t = -\gamma B_t dt + c \frac{1}{2} dW_t,$$

where $\gamma = \frac{1}{\tau}$, τ and c are the correlation time and the diffusion constant of the noise, and W_t is a Wiener process. In this case $B^2(t)$ is known as the square-root process, or the Cox-Ingersoll-Ross (CIR) process [59], whose stochastic differential equation is given by

$$dB_t^2 = (c - 2\gamma B_t^2) dt + 2c \frac{1}{2} \sqrt{B_t^2} dW_t.$$

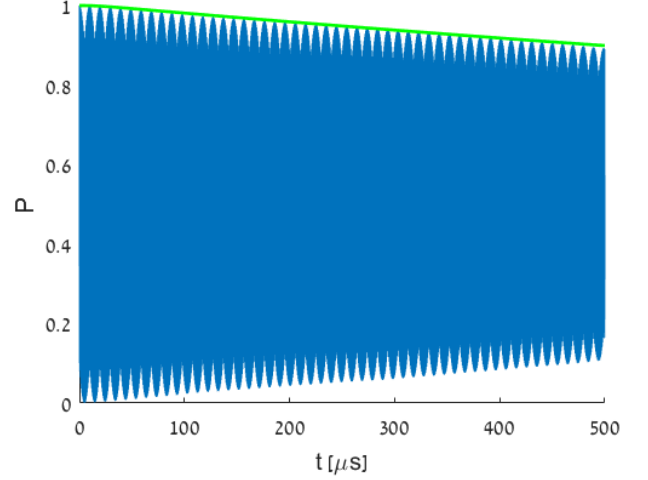


Figure 8. Simulation of the coherence time under a driving of $\Omega = 50$ MHz. Average over 1000 trials. $P_\Omega(t)$ is plotted in green.

Denote the random phase by $\varphi(t) = \frac{1}{\Omega} \int_0^t dt' B^2(t')$. The characteristic function of the square-root process is explicitly given by [59, 60]

$$\left\langle e^{i\varphi(t)} \right\rangle_{B_t^2} = F(t, \Omega) G(t, \Omega),$$

where

$$F(t, \Omega) = \frac{\exp\left(\frac{\gamma t}{2}\right)}{\sqrt{\cosh\left(\frac{\xi t}{2}\right) + \frac{2\gamma}{\xi} \sinh\left(\frac{\xi t}{2}\right)}},$$

$$G(t, \Omega) = \exp\left(\frac{2ig^2}{\Omega \left(2\gamma + \xi \coth\left(\frac{\xi t}{2}\right)\right)}\right),$$

$$\xi = \sqrt{4\gamma^2 - \frac{16i\gamma g^2}{\Omega}},$$

and we assume that $B^2(t=0) = \langle B^2(t) \rangle = g^2 = \frac{c\tau}{2}$.

We therefore conclude that in the strong driving regime, the probability to remain in the initial equal superposition state of the dressed eigenstates is given by

$$P_\Omega(t) = \frac{1 + |F(t, \Omega) G(t, \Omega)|}{2}.$$

We numerically verified this by simulating the noise, $B(t)$, as an Ornstein-Uhlenbeck process with a zero expectation value, $\langle B(t) \rangle = 0$, and a correlation function $\langle B(t) B(t') \rangle = \frac{c\tau}{2} e^{-\gamma|t-t'|}$. An exact simulation algorithm [55] was employed to realize the Ornstein-Uhlenbeck process, which according to

$$B(t + \Delta t) = B(t) e^{-\frac{\Delta t}{\tau}} + n \sqrt{\frac{c\tau}{2} \left(1 - e^{-\frac{2\Delta t}{\tau}}\right)},$$

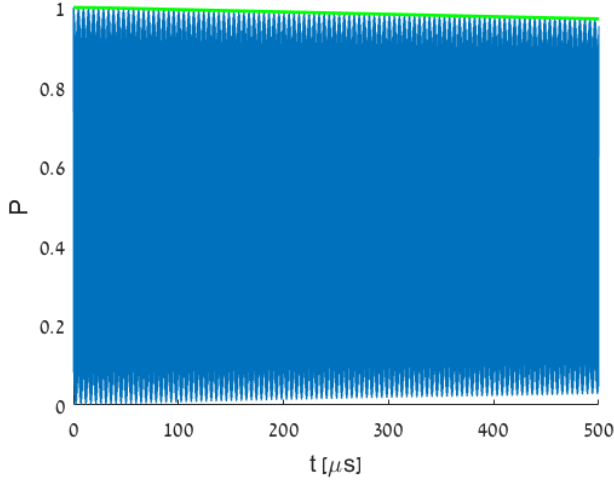


Figure 9. Simulation of the coherence time under a driving of $\Omega = 100$ MHz. Average over 1000 trials. $P_\Omega(t)$ is plotted in green.

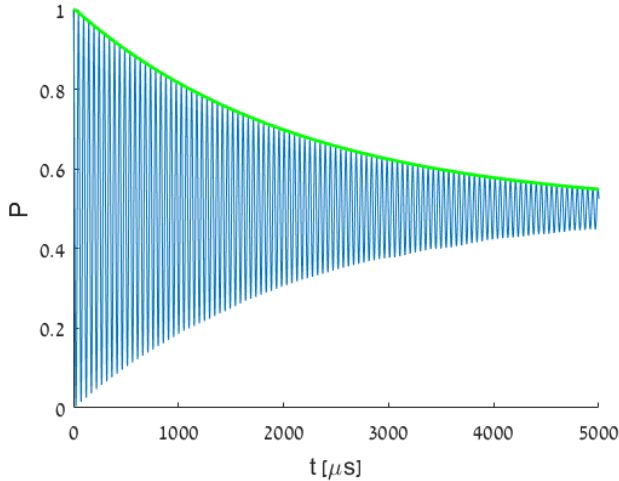


Figure 10. Adiabatic approximation with $\Omega = 50$ MHz. Numerical calculation of $P = \frac{1 + \cos\left(\frac{1}{2} \int_0^t dt' \sqrt{4B^2(t') + \Omega^2}\right)}{2}$. Average over 10000 trials. $P_\Omega(t)$ is plotted in green.

where n is a unit Gaussian random number. We took the pure dephasing time to be $T_2^* = 3 \mu s$, and the correlation time of the noise was set to $\tau = 25 \mu s$. The diffusion constant was therefore given by $c \approx \frac{4}{T_2^{*2} \tau}$. In Fig. 7 the pure dephasing (no driving) is plotted. Then, for two values of Ω , $\Omega = 50$ MHz and $\Omega = 100$ MHz we simulated the time evolution of the TLS, which is initialized to $|\uparrow_z\rangle$, the equal superposition of the dressed eigenstates. Fig. 8 and Fig. 9 show the probability of remaining in the initial state as a function of time. The analytical expression of $P_\Omega(t)$ is plotted in green. In addition, we numerically calculated this probability, which by the adiabatic approximation is given by $P = \frac{1 + \cos\left(\frac{1}{2} \int_0^t dt' \sqrt{4B^2(t') + \Omega^2}\right)}{2}$. In Fig. 10 and Fig. 11 P is plotted as a function of time

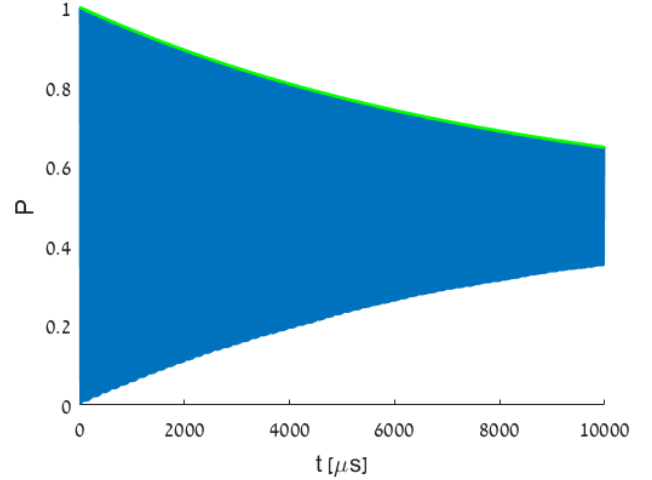


Figure 11. Adiabatic approximation with $\Omega = 100$ MHz. Numerical calculation of $P = \frac{1 + \cos\left(\frac{1}{2} \int_0^t dt' \sqrt{4B^2(t') + \Omega^2}\right)}{2}$. Average over 10000 trials. $P_\Omega(t)$ is plotted in green.

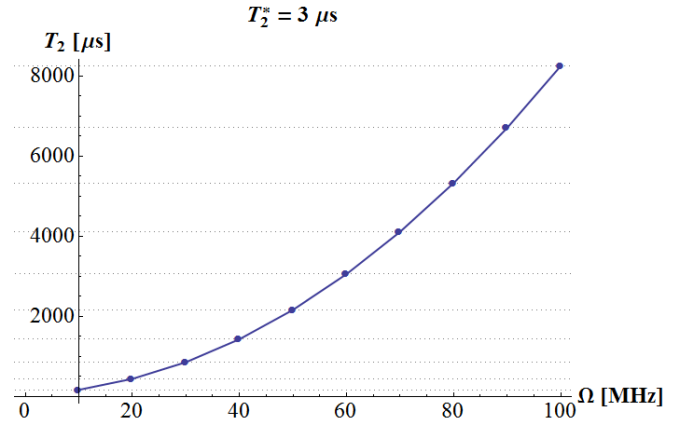


Figure 12. T_2 as function of Ω . The coherence times were deduced by setting $P_\Omega(t) = \frac{1+1/e}{2}$.

and agrees with the analytical expression of $P_\Omega(t)$, which is plotted in green. Increasing Ω increases T_2 . Indeed, a $T_2 = \{167, 857, 2163, 4110, 6707\} \mu s$ is obtained with a driving of $\Omega = \{10, 30, 50, 70, 90\}$ MHz respectively. If Fig. 12 we plot T_2 as function of Ω .

Appendix B

The robustness of the scheme to external noise depends on the energy gap between the dressed states, and can, in principle, be improved by increasing both the Rabi frequency of the driving fields and the detuning Δ . As these are limited, an improvement can be achieved by a double-drive, where in the first drive on-resonance driving fields are applied. The energy gap of the dressed states, which are immune to external noise, is now $\sim \Omega$ (compared to an energy gap of $\frac{\Omega^2}{\Delta}$ in the case of

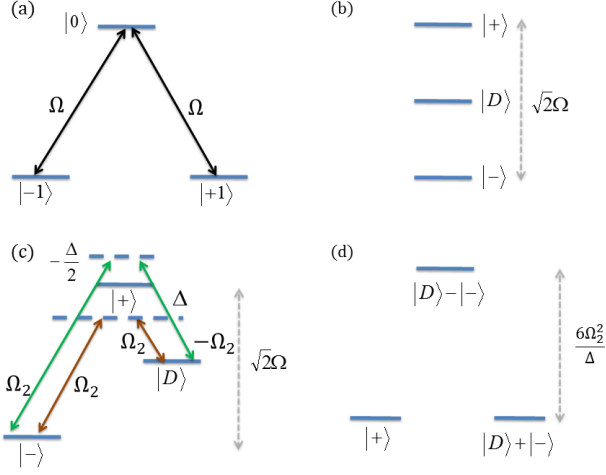


Figure 13. **Improving robustness by a double-drive.** The first on-resonance driving in the bare states basis (a), and the obtained dressed states (b), which are immune to magnetic field fluctuations. (c) Off-resonance driving fields in the dressed states basis and in the first IP, which result in the effective S_x^2 Hamiltonian. (d) Doubly-dressed states. The Stark shifts of the $|+\rangle$ and $|D\rangle+|-\rangle$ states are identical.

a single off-resonance driving) (see Fig. 6 (a),(b)). Next, we add off-resonance driving fields, which results in an effective S_x^2 Hamiltonian of the dressed states, and thus achieves robustness to controller noise as well (see Fig. 13 (c),(d)). In the IP, and taking the RWA, the Hamiltonian of the on-resonance driving fields is given by

$$H_I = \Omega S_x = \sqrt{2}\Omega (|0\rangle\langle B| + |B\rangle\langle 0|). \quad (\text{B1})$$

Its eigenstates and eigenvalues are given by $\left\{ |+\rangle = \frac{1}{\sqrt{2}} (|B\rangle + |0\rangle), |D\rangle, |-\rangle = \frac{1}{\sqrt{2}} (|B\rangle - |0\rangle) \right\}$ and $\left\{ \frac{\Omega}{\sqrt{2}}, 0, -\frac{\Omega}{\sqrt{2}} \right\}$ respectively. Note that all three eigenstates are immune to external noise. In order to construct an effective S_x^2 (or S_y^2) driving Hamiltonian of these dressed states, we first need to construct the couplings $|-\rangle\langle +| + |+\rangle\langle -|$ and $|D\rangle\langle +| + |+\rangle\langle D|$ as building blocks, and then use these for the construction of two off-resonance Λ systems, as in the single-drive scheme (see Fig. 2). By adjusting the phases of the driving fields, which correspond to the $| - 1 \rangle \leftrightarrow | 0 \rangle$ and $| + 1 \rangle \leftrightarrow | 0 \rangle$ transitions, the coupling $i(| - 1 \rangle \langle 0| + | + 1 \rangle \langle 0|) + h.c.$ can be constructed. Moving to the dressed states basis, this results in a $i(| - \rangle \langle +| - | + \rangle \langle -|)$ coupling. Similarly, by adjusting the phases, the $|D\rangle\langle 0| + |0\rangle\langle D|$ coupling is achieved, and adding a phased-matched S_z term results in the desired $|D\rangle\langle +| + |+\rangle\langle D|$ coupling. Hence, an effective S_x^2 Hamiltonian for the dressed states can now be obtained. Alternatively, it can be shown that the effective Hamiltonian, which in the bare states basis is given by

$$H_{eff} = \frac{\Omega_2^2}{\Delta} \left(S_z^2 \cos^2\left(\frac{\Omega}{\sqrt{2}}t\right) S_y^2 \sin^2\left(\frac{\Omega}{\sqrt{2}}t\right) + \frac{\sin(\sqrt{2}\Omega t)}{2\sqrt{2}} (S_y^{-1} - S_y^{+1}) \right), \quad (\text{B2})$$

where $S_y^{-1} = -i|-1\rangle\langle 0| + h.c.$ and $S_y^{+1} = i|+1\rangle\langle 0| + h.c.$, results in $H_{II} = \frac{\Omega_2^2}{\Delta} S_x^2$ in the dressed states basis, when moving to the dressed states basis and to the IP with respect to $H_I = \Omega S_z$. H_{eff} can be constructed with off-resonance driving fields, similar to the single-drive construction.

Appendix C

In Fig. 14 we show the effect of the different sources of noise on the coherence time, which together result in $T_2 = 1820 \mu\text{s}$.

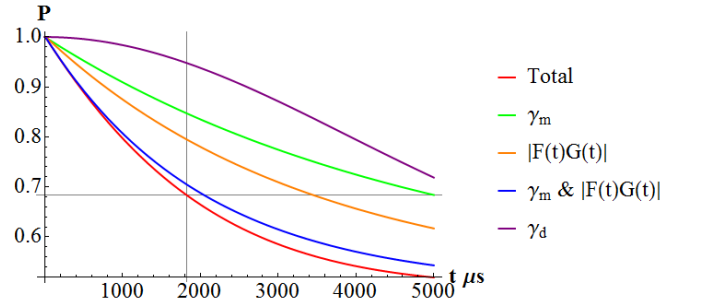


Figure 14. P as function of t . $\gamma_m \approx 200$ Hz - first order dephasing rate due to magnetic noise (green), $|F(t)G(t)|$ - second order dephasing due to magnetic noise (orange), and $\gamma_d = 182$ Hz - dephasing rate due to noise in the driving fields (purple). The total probability to remain in the initial state (red) is given by $P = \frac{1 + |F(t)G(t)| e^{-\gamma_m t} e^{-(\gamma_d t)^2}}{2}$ (See Eq. 17). Gridlines at $P = \frac{1+1/e}{2}$ and $t = 1820 \mu\text{s}$.

Appendix D

Here we give the values of the parameters used in the estimation of T_2 in the case of $T_2^* = 3 \mu\text{s}$. We assume that in all cases we can find a robust point such that $\gamma_d = 285$ Hz (compared to $\gamma_d = 182$ Hz of the simulation).

$g\mu_B B$ (GHz)	Ω (MHz)	Δ_1 (MHz)	γ_d (Hz)
10	60	300	285
20	60	300	285
30	75	400	285
40	85	450	285
50	100	500	285

- [1] E. L. Hahn, *Phys. Rev.* **80**, 580 (1950).
- [2] H. Y. Carr and E. M. Purcell, *Phys. Rev.* **94**, 630 (1954).
- [3] S. Meiboom and D. Gill, *Rev. Sci. Instrum.* **29**, 688 (1958).
- [4] L. Viola and S. Lloyd, *Phys. Rev. A* **58**, 2733 (1998).
- [5] M. J. Biercuk, H. Uys, A. P. VanDevender, N. Shiga, W. M. Itano, and J. J. Bollinger, *Nature* **458**, 996 (2009).
- [6] J. Du, X. Rong, N. Zhao, Y. Wang, J. Yang and R. B. Liu *Nature* **461** 1265 (2009).
- [7] G. de Lange, Z. H. Wang, D. Ristè, V. V. Dobrovitski, and R. Hanson *Science* **330**, 60 (2010).
- [8] C. A. Ryan, J. S. Hodges, and D. G. Cory, *Phys. Rev. Lett.* **105**, 200402 (2010).
- [9] B. Naydenov, F. Dolde, L. T. Hall, C. Shin, H. Fedder, L. C. L. Hollenberg, F. Jelezko, and J. Wrachtrup, *Phys. Rev. B* **83**, 081201(R) (2011).
- [10] Z.-H. Wang, G. de Lange, D. Ristè, R. Hanson, and V. V. Dobrovitski, *Phys. Rev. B* **85**, 155204 (2012).
- [11] N. Bar-Gill, L.M. Pham, A. Jarmola, D. Budker, and R.L. Walsworth, *Nat. Commun.* **4**, 1743 (2012).
- [12] K. Khodjasteh and D. A. Lidar, *Phys. Rev. Lett.* **95**, 180501(2005).
- [13] G. Uhrig, *Phys. Rev. Lett.* **98**, 100504 (2007).
- [14] A. M. Souza, G. A. Álvarez, and D. Suter, *Phys. Rev. Lett.* **106**, 240501 (2011).
- [15] Wen Yang, Zhen-Yu Wang, Ren-Bao Liu, *Front. Phys.* **6**, 2 (2011).
- [16] D. Farfurnik, A. Jarmola, L. M. Pham, Z. H. Wang, V. V. Dobrovitski, R. L. Walsworth, D. Budker, and N. Bar-Gill, *Phys. Rev. B* **92**, 060301(R) (2015).
- [17] Goren Gordon, Gershon Kurizki, and Daniel A. Lidar, *Phys. Rev. Lett.* **101**, 010403 (2008).
- [18] F. F. Fanchini, J. E. M. Hornos, and R. d. J. Napolitano, *Phys. Rev. A* **75**, 022329 (2007).
- [19] A. Bermudez, F. Jelezko, M. B. Plenio, and A. Retzker, *Phys. Rev. Lett.* **107**, 150503 (2011).
- [20] A. Bermudez, P. O. Schmidt, M. B. Plenio, and A. Retzker, *Phys. Rev. A* **85**, 040302(R) (2012).
- [21] J.-M., Cai, F. Jelezko, N. Katz, A. Retzker, and M.B Plenio, *New J. Phys.* **14**, 093030 (2012).
- [22] X. Xu, Z. Wang, C. Duan, P. Huang, P. Wang, Y. Wang, N. Xu, X. Kong, F. Shi, X. Rong, and J. Du, *Phys. Rev. Lett.* **109**, 070502 (2012).
- [23] D.A. Golter, T.K. Baldwin, H. Wang, *Phys. Rev. Lett.* **113**, 237601 (2014).
- [24] P. Rabl, P. Cappellaro, M. V. Gurudev Dutt, L. Jiang, J. R. Maze, and M. D. Lukin, *Phys. Rev. B* **79**, 041302 (2009).
- [25] Jens Clausen, Guy Bensky, and Gershon Kurizki, *Phys. Rev. Lett.* **104**, 040401 (2010).
- [26] V. V. Mkhitarian and V. V. Dobrovitski, *Phys. Rev. B* **89**, 224402 (2014).
- [27] V. V. Mkhitarian, F. Jelezko, and V. V. Dobrovitski, *Sci. Rep.* **5**, 15402 (2015).
- [28] J.-M. Cai, B. Naydenov, R. Pfeiffer, L. P. McGuinness, K. D. Jahnke, F. Jelezko, M. B. Plenio and A. Retzker, *New J. Phys.* **14** 113023 (2012).
- [29] I. Cohen, S. Weidt, W. K. Hensinger, and A. Retzker, *New J. Phys.* **17**, 043008 (2015).
- [30] Jean Teissier, Arne Barfuss, Patrick Maletinsky, [arXiv:1611.01515](https://arxiv.org/abs/1611.01515)
- [31] N. Timoney, I. Baumgart, M. Johanning, A. F. Varón, M. B. Plenio, A. Retzker and Ch. Wunderlich, *Nature* **476**, 185 (2011).
- [32] N. Aharon, M. Drewsen, and A. Retzker, *Phys. Rev. Lett.* **111**, 230507 (2013).
- [33] I. Cohen and A. Retzker, *Phys. Rev. Lett.* **112**, 040503 (2014).
- [34] Z.-Y. Wang *et al.*, *New J. Phys.* **16** 083033 (2014).
- [35] I. Cohen, P. Richerme, Z.-X. Gong, C. Monroe, and A. Retzker, *Phys. Rev. A* **92**, 012334 (2015).
- [36] G. Mikelsons, I. Cohen, A. Retzker, M. B. Plenio, *New J. Phys.* **17**, 053032 (2015).
- [37] T. R. Tan, J. P. Gaebler, R. Bowler, Y. Lin, J. D. Jost, D. Leibfried, and D. J. Wineland, *Phys. Rev. Lett.* **110**, 263002 (2013).
- [38] S. C. Webster, S. Weidt, K. Lake, J. J. McLoughlin, and W. K. Hensinger, *Phys. Rev. Lett.* **111**, 140501 (2013).
- [39] J. Randall, S. Weidt, E. D. Standing, K. Lake, S. C. Webster, D. F. Murgia, T. Navickas, K. Roth, and W. K. Hensinger, *Phys. Rev. A* **91**, 012322 (2015).
- [40] I. Baumgart, J.-M. Cai, A. Retzker, M. B. Plenio, and Ch. Wunderlich, *Phys. Rev. Lett.* **116**, 240801 (2016).
- [41] D. F. James and J. Jerke, *Canadian Journal of Physics*, **85**, 625 (2007).
- [42] Note that since we do not make the RWA, the assumption of a narrow band of frequencies, $|\omega_N - \omega_1| \ll \omega_1$, made in Ref. [41] does not hold in this case. This, however, does not effect the validity of the calculation.
- [43] The energy shifts due to the effective coupling between the $|B\rangle$ and $|D\rangle$ states are $\sim \frac{\Omega^2 \Delta}{(g\mu_B B)^2}$, which is ~ 2 orders of magnitude smaller than the leading contributions of the counter-rotating terms of $\sim \frac{\Omega^2}{g\mu_B B}$. We therefore neglect these terms in the calculation of the energy shifts.
- [44] Under a driving fluctuation, $\Omega \rightarrow \Omega + \delta\Omega$, there is always a point of the parameters such that the energy fluctuations of the $|B\rangle$ and $|0\rangle$ states are equal, $\delta E_B = \delta E_0$, in the first order in $\delta\Omega$. We assume that we can find a set of values of the parameters which is close enough to this point.
- [45] M. Chipaux, L. Toraille, C. Larat, L. Morvan, S. Pezzagna, J. Meijer, and T. Debuisschert, *Appl. Phys. Lett.* **107**, 233502 (2015).
- [46] S. Kolkowitz *et al.*, *Science* **347** 1129 (2015)
- [47] LT Hall, *et al.*, *Nature Communications* **7**, 10211, (2016).
- [48] Kimmich, R., and E. Anoardo. *Prog. Nucl. Magn. Reson. Spectrosc.* **44**, 257. (2004)
- [49] F. Jelezko, T. Gaebel, I. Popa, A. Gruber, and J. Wrachtrup, *Phys. Rev. Lett.* **92**, 076401 (2004).
- [50] F. Jelezko, T. Gaebel, I. Popa, M. Domhan, A. Gruber, and J. Wrachtrup, *Phys. Rev. Lett.* **93**, 130501 (2004).
- [51] G. D. Fuchs, V. V. Dobrovitski, D. M. Toyli, F. J. Heremans, D. D. Awschalom, *Science* **326**, 1520 (2009).
- [52] C. Shin, C. Kim, R. Kolesov, G. Balasubramanian, F. Jelezko, J. Wrachtrup, and P.R. Hemmer, *J. Lumin.* **130**, 1635 (2010).
- [53] M. C. Wang and G. E. Uhlenbeck, *Rev. Mod. Phys.* **17**, 323 (1945).
- [54] R. Hanson, V.V. Dobrovitski, A.E. Feiguin, and O. Gywat 2008, *Science* **320**, 352 (2008).
- [55] D.T. Gillespie, *Phys. Rev.E* **54**, 2084 (1996).
- [56] G. de Lange, T. van der Sar, M. Blok, Z.-H.i Wang, V.V. Dobrovitski, and R. Hanson, *Sci. Rep.* **2**, 382 (2012).
- [57] N. Bar-Gill, L.M. Pham, C. Belthangady, D. Le Sage, P. Cappellaro, J.R. Maze, M.D. Lukin, A. Yacoby, and R. Walsworth, *Nat. Commun.* **3**, 858 (2012).

- [58] P. London, P. Balasubramanian, B. Naydenov, L. P. McGuinness, and F. Jelezko *Phys. Rev. A* **90**, 012302 (2014).
- [59] P. Carr, H. Geman, D. B. Madan, and M. Yor, *Mathematical Finance*, **13**, 345 (2003).
- [60] V.V. Dobrovitski, A. E. Feiguin, R. Hanson, and D. D. Awschalom, *Phys. Rev. Lett.* **102**, 237601 (2009).